

Supplemental information

Membrane Position of Ibuprofen Agrees with Suggested Access Path Entrance to Cytochrome P450 2C9 Active Site

Karel Berka,^a Tereza Hendrychová,^a Pavel Anzenbacher,^b Michal Otyepka*^a

^aRegional Centre of Advanced Technologies and Materials, Department of Physical Chemistry, Faculty of Science, Palacky University, 17. listopadu 12, 771 46 Olomouc, Czech Republic

^bDepartment of Pharmacology, Faculty of Medicine and Dentistry, Palacky University, Olomouc, Czech Republic

updated 4. July 2011

Table ST1 – The diffusion coefficient changes upon membrane insertion.

The diffusion coefficients (D) were calculated with Einstein-Stokes equation from the linear part of the mean square displacement of protein within the simulations. The diffusion coefficients given by this study seem to be too big in comparison with experimental data for several reasons: (i) the use of homogenous DOPC membrane, and (ii) a simplified united-atom Berger force field model of the DOPC/SPC membrane/water environment. Even though the calculated diffusion is by order of magnitude bigger than experimental data, we still can conclude that the diffusion of the solubilized CYP in water is quicker than the diffusion of the CYP bound on the membrane.

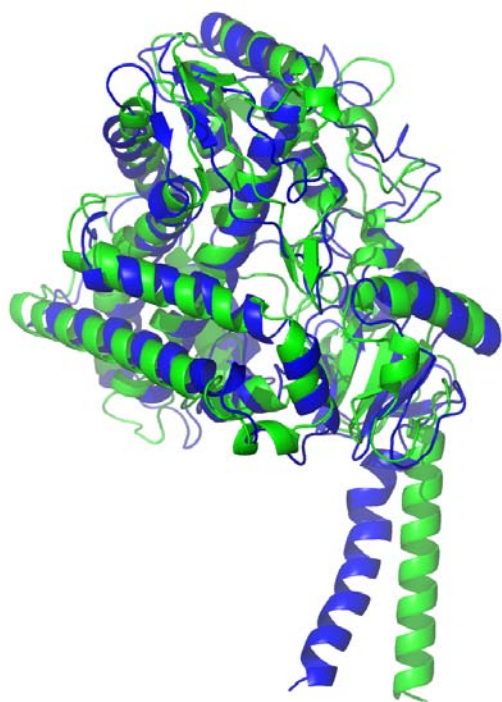
| Diffusion Type and System | Source | D |
|---------------------------------|--------------------|---|
| | | $10^{-7} \text{ cm}^2/\text{s}$ |
| Total, model in water | This study | 7.0 ± 0.26 |
| Total, model in DOPC membrane | This study | 1.6 ± 0.14 |
| Lateral, model in DOPC membrane | This study | 2.1 ± 0.23 |
| Lateral, WALP23 † | Ref. ⁹ | 0.5 ± 0.1 |
| Lateral, CYP2C2 in ER membrane | Ref. ¹⁰ | $5.8 \cdot 10^{-3} \pm 0.2 \cdot 10^{-3}$ |

†artificial helical TM segment in DOPC/DOPG 3:1 membrane.

Figure S2 – Comparison between initial (green) and final (blue) model of wt CYP2C9.

Panel A and B show the protein and membrane changes upon simulation, respectively. The protein is shown in cartoon representation and phosphorous atoms from the membrane are shown as spheres. While the protein core did not change significantly during the simulation, the membrane topology and parts of protein responsible for the interaction with the membrane show slight rearrangement as discussed in paper. The figure was prepared in Pymol 0.99rc6¹¹.

A



B

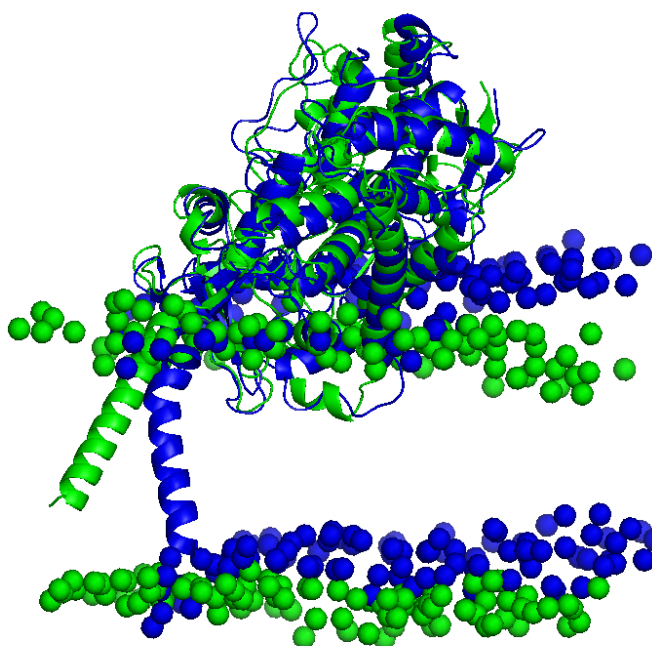


Figure S3 – The evolution of RMSD of CYP2C9 on the membrane in three individual simulations used in selection of the appropriate model.

The simulation was triplicated after first 10 ns. The simulations were then equilibrated after approximately 20 ns.

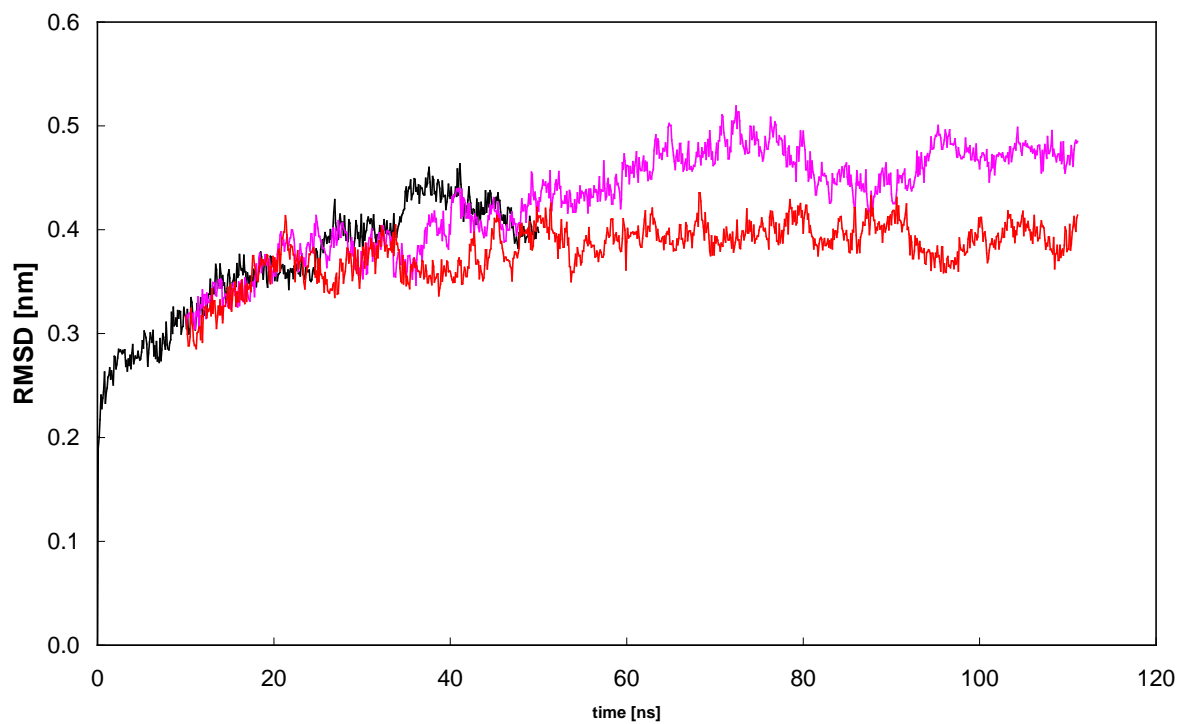


Figure S4 – Detailed structure of the transmembrane helical segment of CYP2C9.

The transmembrane helix is shown in magenta. The N-terminal part is not perpendicular to the membrane, nor is penetrating beyond charged groups in the luminal part of membrane. The helix is kinked in the Arg21 position. The figure was prepared in Pymol 0.99rc6¹¹.

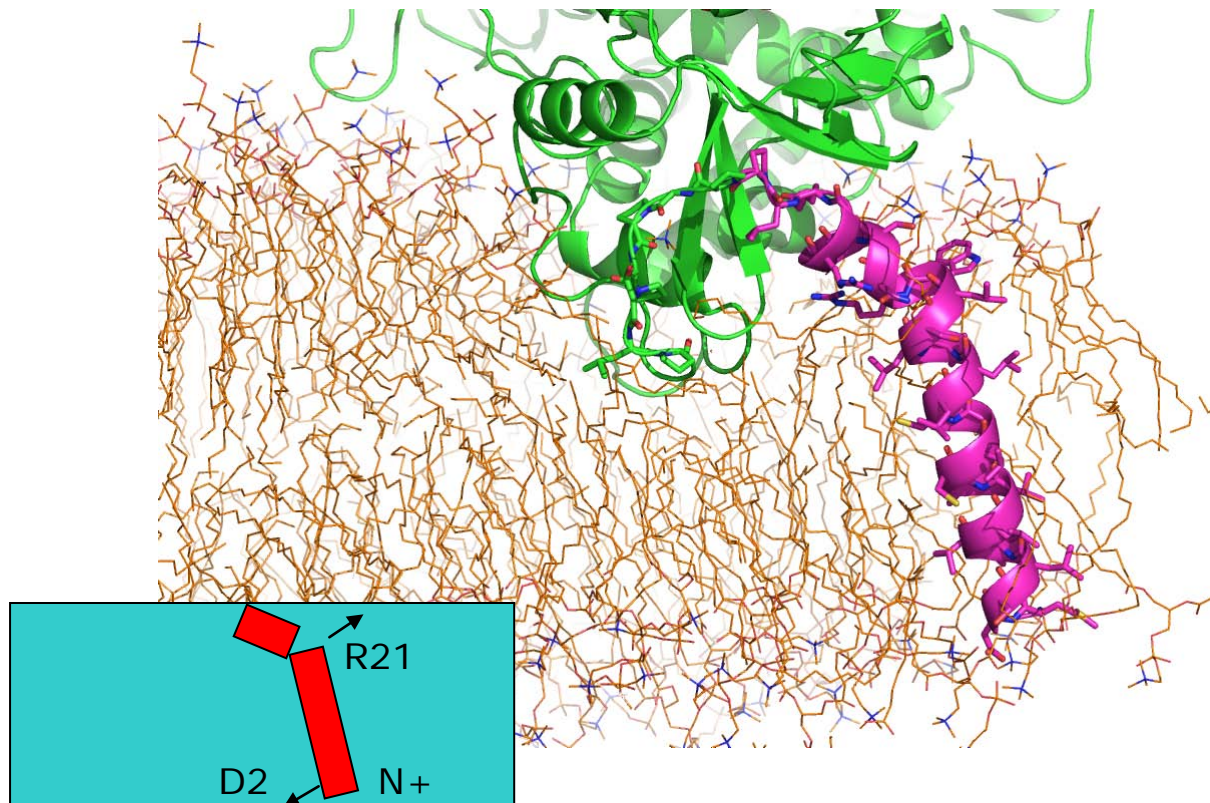


Figure S5 – Channel opening and closing during membrane simulations of CYP2C9.

Channel opening analysis provided by Vlad Cojocaru on our two independent simulations. The most open channel is solvent channel followed to some extent by channels 2c and 2ac as seen in coloring in the picture.

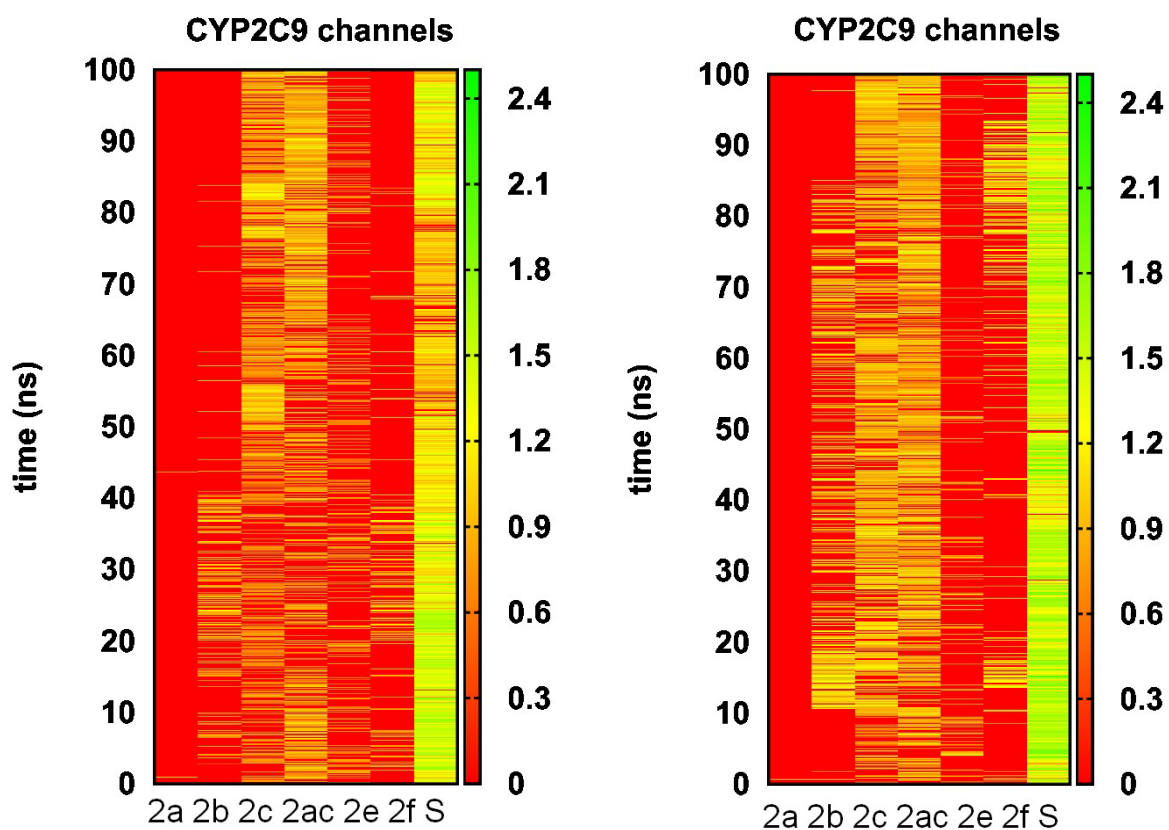
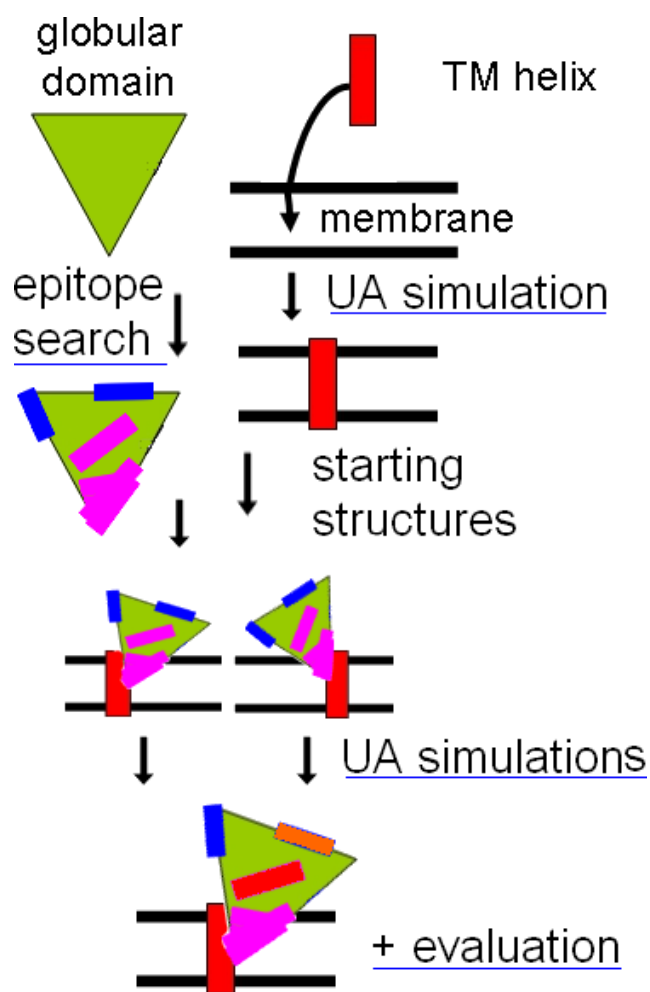


Figure S6 – Schematics of model preparation.

First, position of transmembrane helix in membrane has been evaluated by short 10 ns united atom simulation. The transmembrane helix was shown to be almost perpendicular to the membrane normal. Secondly, the starting positions of the globular domain were selected upon epitope labeling and the globular domain was merged to the transmembrane helix. After that three parallel simulations were produced with united atom force field for total time of 250 ns. Final model was then compared to all known experimental data as shown in the section *Final model cross-validation* in the Results.



References

- (1) Larkin, M. A.; Blackshields, G.; Brown, N. P.; Chenna, R.; McGettigan, P. A.; McWilliam, H.; Valentin, F.; Wallace, I. M.; Wilm, A.; Lopez, R.; Thompson, J. D.; Gibson, T. J.; Higgins, D. G. *Bioinformatics*. **2007**, *23*, 2947-8.
- (2) Waterhouse, A. M.; Procter, J. B.; Martin, D. M. a; Clamp, M.; Barton, G. J. *Bioinformatics*. **2009**, *25*, 1189-91.
- (3) Bridges, A.; Gruenke, L.; Chang, Y. T.; Vakser, I. A.; Loew, G.; Waskell, L. *J. Biol. Chem.* **1998**, *273*, 17036-49.
- (4) Black, S. D.; Martin, S. T.; Smith, C. A. *Biochemistry*. **1994**, *33*, 6945-51.
- (5) Black, S. D. *The FASEB Journal*. **1992**, *6*, 680-685.
- (6) Wachenfeldt, C. von; Johnson, E. F. In *Cytochrome P450: Structure, Mechanism, and Biochemistry*; Plenum Press: New York, 1995; p. 183–244.
- (7) Cosme, J.; Johnson, E. F. *J. Biol. Chem.* **2000**, *275*, 2545-2553.
- (8) Williams, P. A.; Cosme, J.; Ward, A.; Angove, H. C.; Matak Vinković, D.; Jhoti, H. *Nature*. **2003**, *424*, 464-8.
- (9) Ramadurai, S.; Holt, A.; Krasnikov, V.; Bogaart, G. van den; Killian, J. A.; Poolman, B. *J. Am. Chem. Soc.* **2009**, *131*, 12650-6.
- (10) Szczesna-Skorupa, E.; Chen, C. D.; Rogers, S.; Kemper, B. *Proc. Natl. Acad. Sci. USA*. **1998**, *95*, 14793-8.
- (11) DeLano, W. L. *The PyMOL Molecular Graphics System*, <http://pymol.org>, 0.99rc6; DeLano Scientific: Palo Alto, CA, USA, **2002**.